2025 S.T. Yau High School Science Award (Asia)

Research Report

The Team

Registration Number: Chem-029

Name of team member: Adviteeya Krishna
School: NUS High School of Mathematics & Science
Country: Singapore

Name of team member: Logan Wong Duran
School: NUS High School of Mathematics & Science
Country: Singapore

Name of supervising teacher: Murali Krishnaswamy
Job Title: Chemistry Teacher
School: NUS High School of Mathematics & Science
Country: Singapore

From Atoms to Armor: Sustainable Multilayered Nanocomposites for

Effective Radiation Shielding

Date

14 August 2025

From Atoms to Armor: Sustainable Multilayered Nanocomposites for Effective Radiation Shielding

Logan Wong Duran, Adviteeya Krishna

Abstract

The global demand for radiation-based diagnostics and therapy is increasing rapidly, with projections estimating over 84 million individuals requiring radiotherapy by 2050. To protect medical personnel from ionizing radiation, lead-based aprons have long been the standard. While effective at radiation attenuation, lead suffers significant drawbacks, including its high toxicity, substantial weight, environmental hazards, and significant challenges in long-term waste management after disposal.

In this study, we address these limitations by developing a novel multilayered polymer nanocomposite for effective radiation shielding, integrating various nanoparticles into a thermoplastic matrix. Specifically, gadolinium oxide (Gd_2O_3), zirconium oxide (ZrO_2), and bismuth (Bi) nanoparticles were dispersed in High-density Polyethylene (HDPE) to maximize both photon and neutron attenuation. Unlike conventional lead aprons, our nanocomposite offers a lightweight, non-toxic, and flexible alternative with tailored shielding performance. Moreover, thermoplastics offer the advantage of recyclability at the end of their lifespan, aligning with sustainability goals.

To create a wearable nanocomposite, we synthesized and investigated the effects of nanoparticle morphology and its composition on both shielding performance and mechanical integrity. Our In-house synthesis enabled precise control and to benchmark our nanoparticles against commercial equivalents. Through melt-blown processing, we fabricated a flexible multi-layered woven sheet, which was subsequently assembled into a prototype for a wearable PPE.

Our study presents a scalable methodology for fabricating a novel multi-layered radiation shielding nanocomposite that is sustainable, lightweight, and can be made into comfortable apparel.

Keywords: nanocomposites, polymer composites, sustainable materials, nanoparticles, radiation shielding, medical protection

Acknowledgement

1) We are eternally grateful to our research mentor, Dr. Ice Tee Si Yin, for her constant support, guidance, and encouragement throughout our research journey.

2) We are grateful to our school chemistry teacher, Mr. Murali Krishnaswamy, for checking in with us throughout our research journey and being supportive of our endeavors.

3) We are grateful to A*STAR Institute of Materials Research and Engineering (IMRE) for providing us with the laboratory facilities and resources to conduct our novel project.

4) We are grateful to our friends and families for motivating us and supporting us throughout our research journey.

Commitments on Academic Honesty and Integrity

We hereby declare that we

1. are fully committed to the principle of honesty, integrity and fair play throughout the competition.
2. actually perform the research work ourselves and thus truly understand the content of the work.
3. observe the common standard of academic integrity adopted by most journals and degree theses.
4. have declared all the assistance and contribution we have received from any personnel, agency, institution, etc. for the research work.
5. undertake to avoid getting in touch with assessment panel members in a way that may lead to direct or indirect conflict of interest.
6. undertake to avoid any interaction with assessment panel members that would undermine the neutrality of the panel member and fairness of the assessment process.
7. observe the safety regulations of the laboratory(ies) where the we conduct the experiment(s), if applicable.
8. observe all rules and regulations of the competition.
9. agree that the decision of YHSA(Asia) is final in all matters related to the competition.

We understand and agree that failure to honour the above commitments may lead to disqualification from the competition and/or removal of reward, if applicable; that any unethical deeds, if found, will be disclosed to the school principal of team member(s) and relevant parties if deemed necessary; and that the decision of YHSA(Asia) is final and no appeal will be accepted.

(Signatures of full team below)

Name of team member: Adviteeya Krishna

Name of team member: Logan Wong Duran

Name of supervising teacher: Mr Murali Krishnaswamy

Noted and endorsed by

(signature)

Name of school principal: f. Goh Hock Leong

Table of Contents

4. Conclusion

5. References

1. Introduction

1.1 Background

Advancements in modern medicine and technology have significantly expanded the use of nuclear radiation, offering powerful tools for diagnosing and treating diseases, as well as improving patient outcomes through techniques such as fluoroscopy and radiation therapy. However, prolonged exposure to ionizing radiation, such as gamma rays and X-rays, remains harmful to biological tissues and is often associated with increased risks of cancer, immune disorders, and other long-term health effects. Elements with a high atomic number (Z), like lead, are excellent shields for ionizing radiation as they interact with the rays more. Therefore, lead aprons have long been the standard personal protective equipment (PPE), owing to lead's high Z and exceptional ability to absorb and attenuate high-energy radiation. [1-9]

Despite their effectiveness, lead aprons present notable drawbacks. Interactions between lead and incident radiation can generate secondary gamma emissions, potentially introducing additional risks to the wearer. Moreover, the substantial weight of these aprons imposes significant physical strain, with regular use often linked to musculoskeletal disorders, including chronic back pain and degenerative disc disease. Lead is also a highly toxic metal, which leads to environmental degradation and diseases if not disposed of properly.

These limitations underscore the importance of innovation towards better alternatives for radiation shielding. In this study, a PPE was invented using a novel polymer nanocomposite synthesized by the layering of Bismuth (Bi), Gadolinium (Gd) Oxide and Zirconium (Zr) Oxide nanoparticles (Fig. 1) in a High-Density PolyEthylene (HDPE) matrix to combat these limitations. We controlled the size, morphology, and surface chemistry to ensure optimal compatibility and uniform dispersion within polymer matrices, thus allowing for the development and prototyping of a lightweight, non-toxic PPE for radiation protection.

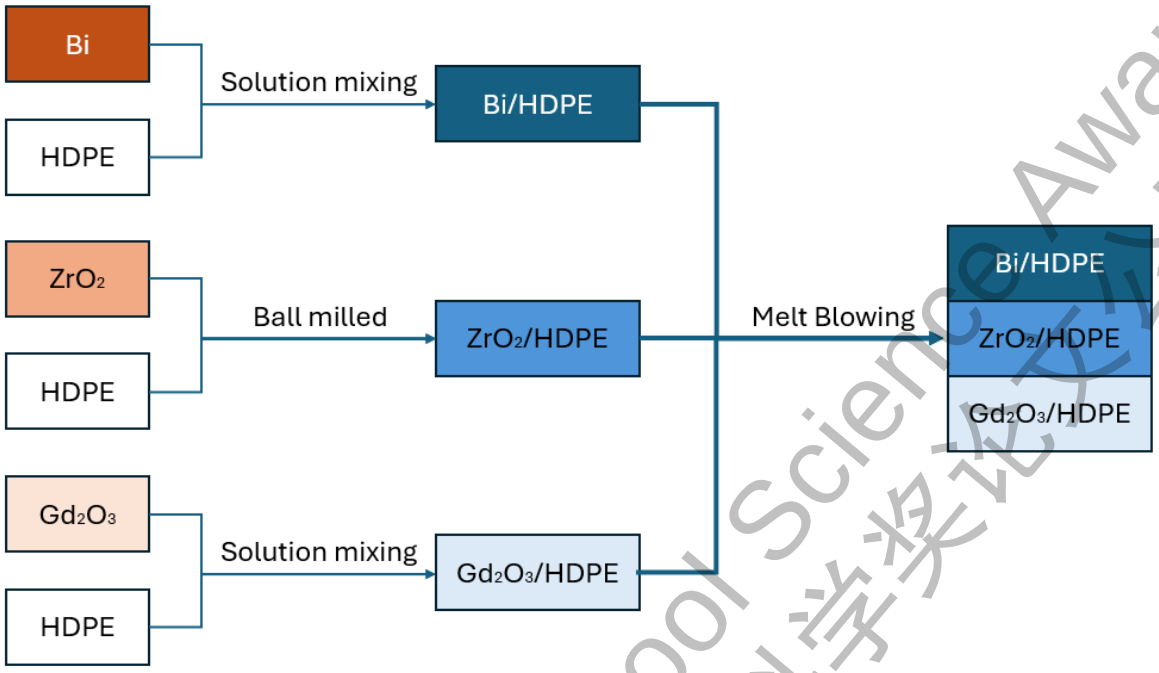

Fig. 1 Process flow diagram showing the fabrication of the multilayered nanocomposite. Bi and Gd_2O_3 nanoparticles were synthesized *via* colloidal methods, while ZrO_2, was obtained commercially. Each nanoparticle type was blended with powdered HDPE to form individual compound layers. These layers were pelletized and subsequently co-extruded using a melt-blown process to produce the final multilayered nanocomposite.

1.2 Literature review

To replace lead-based aprons for medical applications, the use of various nanoparticles incorporated into polymer matrices has been studied.

An example of such is Bismuth. Bi (Z = 83) and its oxide, Bi_2O_3 are being widely studied as lead-free radiation shielding fillers because they pair high atomic number and density with comparatively low toxicity and good chemical stability. Bi_2O_3 has been dispersed into a wide range of polymer matrix composites (PMCs), including but not limited to Poly Methyl Methacrylate (PMMA), epoxies, and silicone or natural rubbers. Having high modulus and melting point, its use is to enhance both the

tensile strength and thermal stability of the polymer nanocomposite. A recent study by Alsaab *et. al.* demonstrated that PMMA/Bi_2O_3 nanocomposites were highly effective for X-ray and gamma-ray shielding, while being safer and more lightweight as compared to today's lead-based radiation shields. [10] The doped polymer matrices showed improved gamma ray shielding ability by as much as 100 keV as compared to pure PMMA. Furthermore, higher weight percentages of Bismuth Oxide showed improved mechanical properties, including hardness of the composites produced. Similarly, Echeweozo *et al.* reported that PMMA doped with 20 wt% Bi_2O_3 (PM-2Bi) achieved mass attenuation coefficients of 20.74818 cm^2/g at 0.015 MeV and 0.02448 cm^2/g at 15 MeV photon energy, confirming its strong shielding efficiency. These findings underscore Bismuth oxide's suitability as a nanofiller for advanced radiation-shielding polymer composites.

Another nanoparticle that has garnered much attention in recent years is Gadolinium. Being an element of high atomic mass (Z = 64), it has shown a promising ability in shielding neutron radiation (with a thermal neutron capture cross-section of approximately 255,000 barns). In a study conducted by Wang *et. al.*, Gd_2O_3 nanoparticles were doped into various PMCs with varying nanoparticle concentration and their performance in shielding neutron radiation was studied. [11] The composite demonstrated a neutron transmittance rate of as low as 35.3% when the Gd_2O_3 nanoparticles were dispersed at 54% by weight of the composite. Similarly, Seyed *et. al.* explored the effects of homogeneously distributing Gd_2O_3 nanoparticles within an epoxy resin. [12] The investigation showed that the dispersion of Gd_2O_3 nanoparticles significantly improves neutron shielding as compared to the neat epoxy resin. At a thickness of 4 cm with just 0.5% Gd_2O_3 content, the composites reduced neutron beam intensity by 54% as compared to the neat epoxy sample, which absorbed 37% of the neutron radiation. thus showcasing its exceptional ability in neutron shielding.

Subsequently, another metal being studied is Zirconium. It is a high-Z (Z = 40) metal that has high strength and chemical stability. Its oxide is non-toxic and sustainable, while being cost-effective and

offering high radiation attenuation capabilities. [13] Fontainha *et al.* demonstrated its potential by developing a lightweight, flexible, and cost-efficient X-ray shielding material for fluoroscopy. [14] Using a sol–gel synthesis, they dispersed ZrO_2 into a poly(vinylidene fluoride–trifluoroethylene) [P(VDF–TrFE)] copolymer blended with PMMA, achieving a composite containing 10 wt% ZrO_2 that, at just 1.0 mm thickness, attenuated 60% of X-ray radiation.

ZrO_2 can also function synergistically with other high-Z metals. For instance, Alhindawy *et al.* reported a novel one-step sol–gel fabrication method to produce lead dioxide (PbO_2)-doped zirconia. They observed that decreasing crystallite size increased both PbO_2 content and radiation-shielding efficiency, with the composite outperforming pure lead. [15] Furthermore, ZrO_2's photon absorption capabilities at low emission levels make it particularly relevant to medical settings. Thus, ZrO_2 is a promising nanoparticle for polymer matrix composites with high potential in shielding low-intensity ionising radiation.

The reviewed studies collectively demonstrate that incorporating high-Z nanoparticles such as Bi_2O_3, Gd_2O_3, and ZrO_2 into polymer matrices offers the prospect of a promising future toward developing lightweight, non-toxic, and high-performance alternatives to conventional lead-based radiation shields. Bi_2O_3 offers excellent attenuation of X-rays and gamma rays while enhancing mechanical and thermal properties; Gd_2O_3 provides exceptional neutron shielding owing to its remarkably high thermal neutron capture cross-section; and ZrO_2 delivers effective photon attenuation, particularly at low radiation levels, while maintaining chemical stability and cost-effectiveness. Furthermore, the versatility of these nanofillers across diverse polymer matrices, such as HDPE and PMMA highlights their adaptability for applications is various settings. These findings demonstrate the potential of polymer nanocomposites to address the challenges of multi-type radiation protection in medical settings, paving the way for future materials in advanced radiation shielding.

1.3 Novelty

Existing studies have been largely focused on single-filler composites, which limits the scope of protection to specific radiation types. To address this, we propose the development of a multilayered polymer nanocomposite in which layers containing different nanoparticles are co-extruded into a single sheet, thereby maximizing shielding efficiency across gamma, X-ray, and neutron spectra. Specifically, our design will incorporate Bi_2O_3, Gd_2O_3, and ZrO_2 dispersed within a high-density polyethylene (HDPE) matrix, forming a lightweight, non-toxic, and sustainable shielding material capable of shielding effectively against various types of radiation.

2. Methodology

2.1 Synthesis of Bi Nanoparticles

Bismuth nanoparticles were synthesized *via* a colloidal synthesis route in which a bismuth precursor was dissolved in an organic solvent that also functioned as the reducing agent and stabilizing agent, controlling particle growth and preventing agglomeration. The solution was purged with argon to remove oxygen and moisture, ensuring an inert atmosphere before heating it back to the desired elevated temperature. Nanoparticle formation was indicated by a distinct color change to black, marking nucleation and growth. After the reaction was complete, the mixture was cooled to room temperature, and the resulting nanoparticles were purified through repeated washing and centrifugation prior to further characterization.

2.2 Synthesis of Gd_2O_3 Nanoparticles

Gd_2O_3 nanoparticles were similarly prepared through a colloidal synthesis process by combining a Gd precursor with a solvent and stabilizing agent to achieve controlled particle size and stability. The mixture was degassed under argon to eliminate dissolved gases and moisture, then heated to the target elevated temperature under an inert atmosphere to facilitate nanoparticle formation. Following

the reaction, the solution was cooled to room temperature, and the nanoparticles were isolated and purified through multiple washing and centrifugation cycles before proceeding to detailed characterization.

2.3 Synthesis of ZrO_2 Particles

Zirconium oxide was purchased and used directly from Sigma Aldrich.

2.4 Preparation of HDPE Powder

HDPE Pellets were dissolved in toluene using a silicon oil bath at high temperatures. Thereafter, it was powdered using a blender.

2.5 Layering of Nanocomposites

For Bi Nanoparticles, it was ball milled with a capping agent and the HDPE powder. Thereafter, it was extruded and pelletized. For Gd_2O_3 Nanoparticles, a melt-blending technique was utilized to evenly and homogenously distribute the nanoparticles within the HDPE matrix. For ZrO_2, similar processes to Bismuth were conducted. After the pellets were obtained, some were sectioned off to be melt blown into a thin sheet of multilayered polymer nanocomposites. The rest was injection molded into impact and tensile bars, as shown in Fig 2.

Fig 2. The impact bars of (a) ZrO_2, (b) Gd_2O_3, and (c) Bi tensile bars.

2.6 Characterization

2.6.1 X-Ray Diffraction Analysis

To assess phase purity and obtain detailed information on the crystalline structure of our in-house synthesized nanoparticles, we conducted X-Ray Diffraction (XRD) analyses. The diffraction patterns obtained were compared against reference data from the International Centre for Diffraction Data (ICDD) database to verify phase identity and detect the presence of any secondary or impurity phases.

2.6.2 Electron Microscopy Analysis

Through detailed analysis of Scanning Electron Microscopy (SEM) and Transmission Electron Microscopy (TEM) images, we obtained a deeper understanding of the morphology, size distribution, and dispersion characteristics of the in-house synthesized nanoparticles. SEM imaging was employed to assess particle distribution and overall morphology, while TEM imaging provided higher-resolution analysis of nanoscale dimensions, surface smoothness, and potential agglomeration. Both techniques were applied to evaluate the uniformity of particle synthesis and to verify the effectiveness of stabilizing agents in reducing aggregation during colloidal synthesis.

2.7 Mechanical Tests

2.7.1 Tensile

Tensile strength measurements were conducted on polymer matrix composite specimens prepared in a standard dog bone geometry by a Minijet Injection Molding machine. The test measured the maximum stress sustained before fracture, allowing us to evaluate the composite's ultimate tensile strength and elongation at break.

2.7.2 Impact

Composite samples were prepared in standard bar geometry and notched to a depth of 0.0025m to

promote controlled fracture. A pendulum hammer was released to strike the notched sample, and the energy absorbed during fracture was determined from the difference in the hammer's starting and ending swing heights. This allowed us to quantify the material's toughness.

3. Results and Discussion

3.1 Colloidal Synthesis of Nanoparticles

In this project, we employed a colloidal synthesis to prepare Bi and Gd nanoparticles using a bottom-up approach involving four key components: a metal precursor, solvent, reducing agent, and stabilizing agent. Typical metal precursors include ionic salts such as nitrates, chlorides, sulfates, acetates, and acetylacetonates, like what was done in this experiment. During synthesis, the stabilizing agent adsorbs on the nanoparticle surface, forming a protective shell that serves two main functions: (i) controlling nanoparticle growth by regulating precursor diffusion from the surrounding solution into the particle core, and (ii) preventing agglomeration through steric, electrostatic, or electrosteric stabilization.

Due to these growth-controlling and stabilizing effects, stabilizing agents adsorb onto the nanoparticle surface and inhibit coalescence by introducing steric hindrance between similarly protected particles. Ligand-based stabilization is another widely used strategy, in which molecules containing functional groups such as thiols, amines, organic acids, or phosphines coordinate via their heteroatoms to the metal atoms on the nanoparticle surface. This coordination provides robust steric stabilization while also enabling surface functionalization, which can be tailored for improved dispersion in polymers or for specific chemical reactivity in subsequent applications (Fig. 3).

The particle size, morphology, and surface chemistry were tuned to ensure homogeneous dispersion within HDPE and to promote strong interfacial interactions with the polymer matrix. This optimization maximizes the combined photon- and neutron-shielding performance of the resulting multilayered

polymer nanocomposites, enabling a lightweight, flexible, and lead-free alternative for radiation protection application.

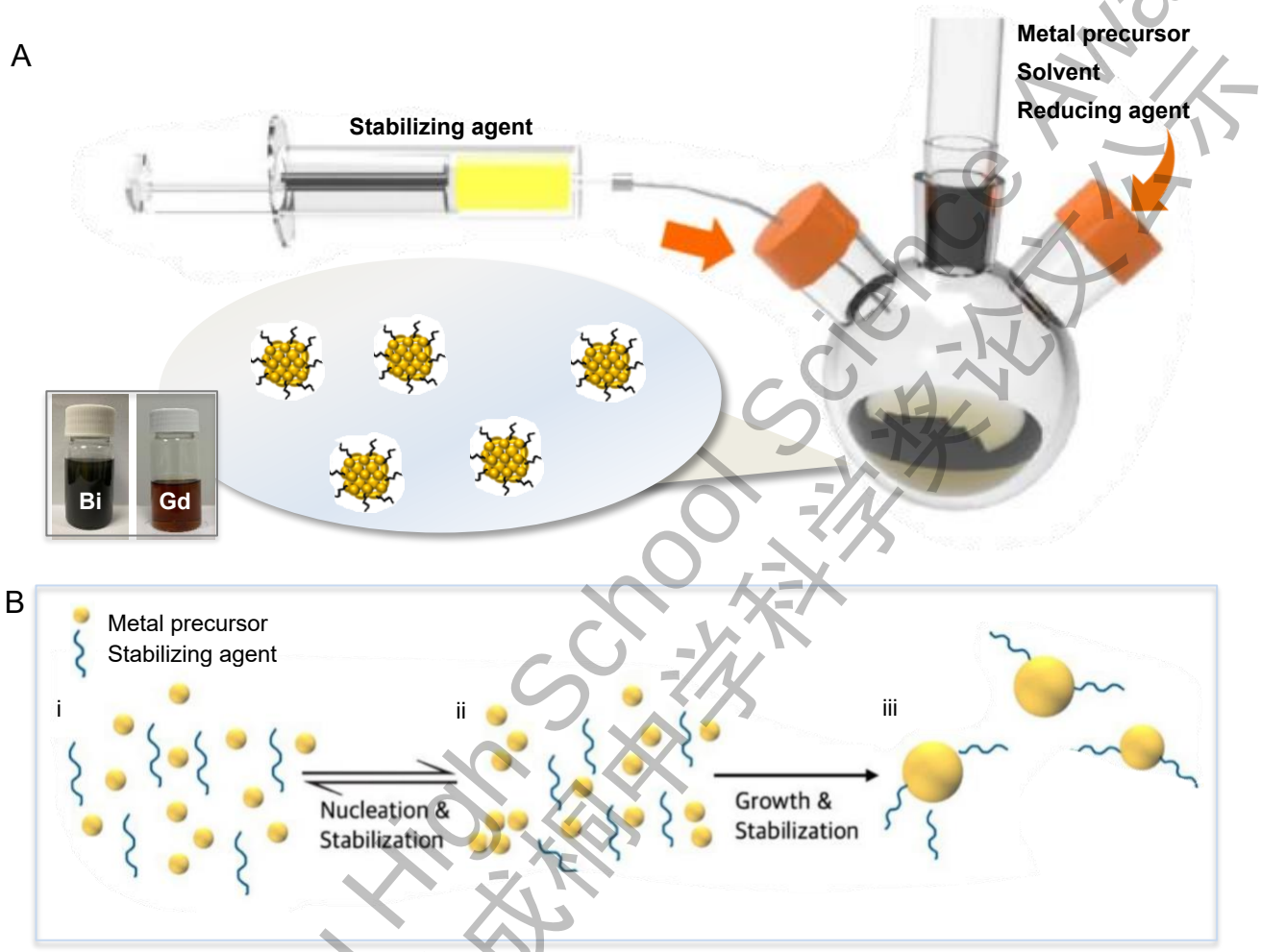

Fig. 3 Synthesis of Bi nanoparticles and Gd_2O_3 nanoparticles using colloid synthesis. (A) Schematic illustration of the synthesis routes, including chemical reduction and thermal decomposition. In these colloidal processes, a stabilizing or capping agent is used to control nucleation and growth, prevent aggregation, and enable precise tuning of particle size, morphology, and surface chemistry for incorporation into polymer composites. Inset shows photographs of Bi and Gd_2O_3 nanoparticles dispersed in an organic solvent, illustrating their stable colloidal state. (B) General mechanism of colloidal nanoparticle formation, showing the sequential steps of (i) combining the metal precursor with a stabilizing or capping agent to prevent aggregation, (ii) nucleation and simultaneous stabilization of initial nuclei, and (iii) particle growth with continued stabilization to achieve uniform size and morphology.

3.2 Phase Identification and Crystallinity of Synthesized Nanoparticles

The XRD patterns in Fig. 4 below confirm the successful synthesis and phase purity of the Bi and Gd_2O_3 nanoparticles. The diffraction peaks in Fig. 4A match well with the standard JCPDS Card No. 001-0699, corresponding to rhombohedral bismuth. The sharp and well-defined peaks indicate a high degree of crystallinity in the synthesized Bi nanoparticles. The absence of additional peaks confirms the phase purity, suggesting that the colloidal synthesis process effectively produced single-phase bismuth without detectable impurity phases.

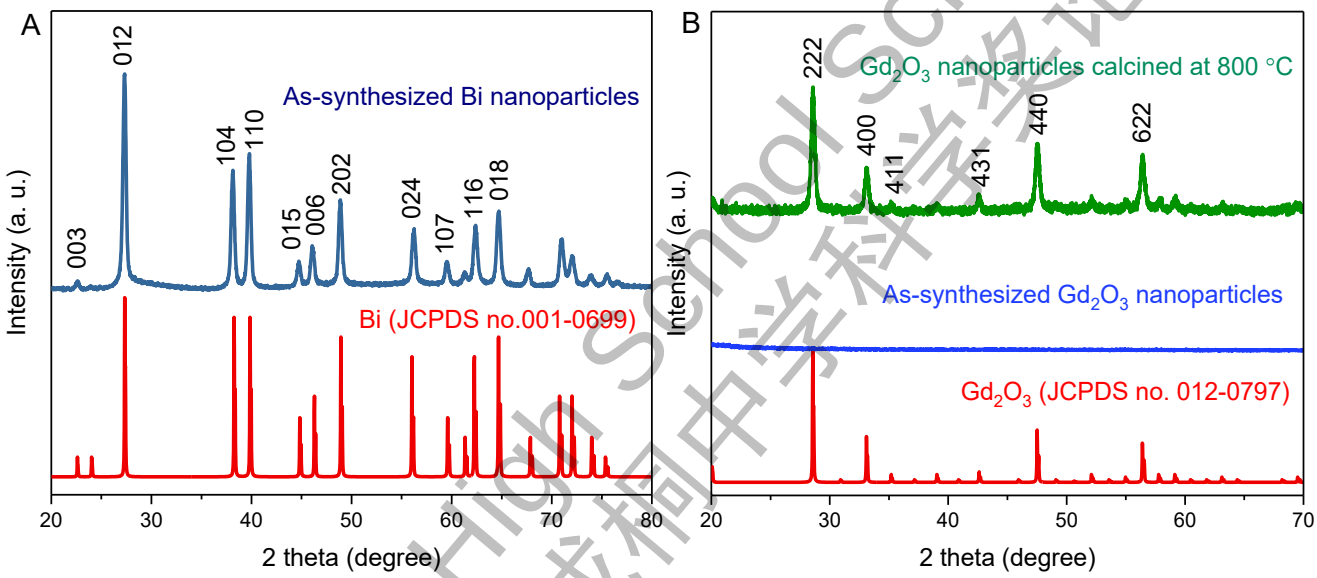

Fig. 4 XRD patterns of (A) as-synthesized Bi nanoparticles, showing diffraction peaks matching JCPDS Card No. 001-0699, and (B) as-synthesized Gd_2O_3 nanoparticles and Gd_2O_3 nanoparticles calcined at 800 °C, with peaks matching JCPDS Card No. 012-0797.

Fig. 4B shows the XRD patterns of as-synthesized and calcined Gd_2O_3 nanoparticles. The as-synthesized sample exhibits a broad hump rather than sharp peaks, characteristic of an amorphous structure with short-range order. After calcination at 800 °C, distinct diffraction peaks appear, matching the cubic phase of Gd_2O_3 (JCPDS Card No. 012-0797). This structural transformation from amorphous to crystalline Gd_2O_3 demonstrates the effect of thermal treatment in promoting crystallinity and phase

development. The narrowing of peaks after calcination further suggests grain growth and improved crystallite ordering.

In the multilayered HDPE-based system, crystalline Bi nanoparticles ensure efficient high-energy photon attenuation, while amorphous Gd_2O_3 provides neutron shielding in a form that enhances dispersion stability and composite toughness. The ability to confirm composition through calcination while preserving amorphous structure in the final product ensures that the fillers combine optimal radiation attenuation with favorable processing and mechanical characteristics.

3.3 Morphological Evaluation and Elemental Mapping of Core–Shell Nanoparticles

The SEM image (Fig. 5A) shows that the Bi nanoparticles are uniformly distributed with an average diameter of approximately 50 nm and a predominantly spherical morphology. This uniformity suggests precise control of nucleation and growth kinetics during the colloidal synthesis process. The TEM image (Fig. 5B) provides higher-resolution confirmation of their nanoscale dimensions and surface characteristics, showing smooth particle surfaces with minimal agglomeration, likely due to the use of stabilizing agents during the colloidal synthesis process.

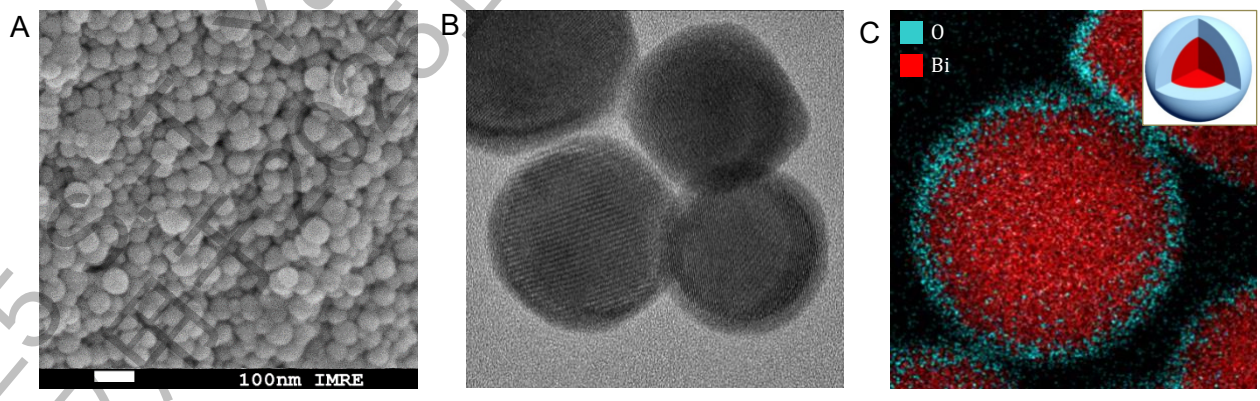

Fig. 5 (A) SEM and (B) TEM images of Bi_2O_3 nanoparticles, showing their morphology and size distribution. (C) TEM–EDX elemental mapping confirming the $Bi@Bi_2O_3$ core–shell architecture, with the inset illustrating the schematic representation of the core–shell structure.

TEM–EDX elemental mapping (Fig. 5C) distinctly confirms the presence of a core–shell architecture, where a metallic Bi core is encapsulated by a Bi_2O_3 shell. The clear spatial separation of Bi and oxygen signals supports the formation of this structure rather than a homogeneous oxide particle. The inset schematic further illustrates this Bi@Bi_2O_3 arrangement, which is particularly advantageous for radiation shielding applications: the dense Bi core offers high-Z photon attenuation, while the Bi_2O_3 shell enhances chemical stability and dispersibility within the polymer matrix. Such a hierarchical design not only improves the interfacial compatibility with the host polymer but also maintains the structural integrity of the nanoparticles during processing and irradiation.

3.4 Impact Strength Optimization in HDPE/Bi Composites

The SEM cross-sectional image (Fig. 6A) confirms that Bi particles are uniformly dispersed within the HDPE matrix, with no evidence of large-scale agglomeration. This homogeneous distribution is critical for maintaining consistent load transfer throughout the composite, reducing the likelihood of localized stress concentrations that could initiate cracks. The inset photograph further supports this observation, showing no visible particle clustering or phase separation at the macroscopic scale.

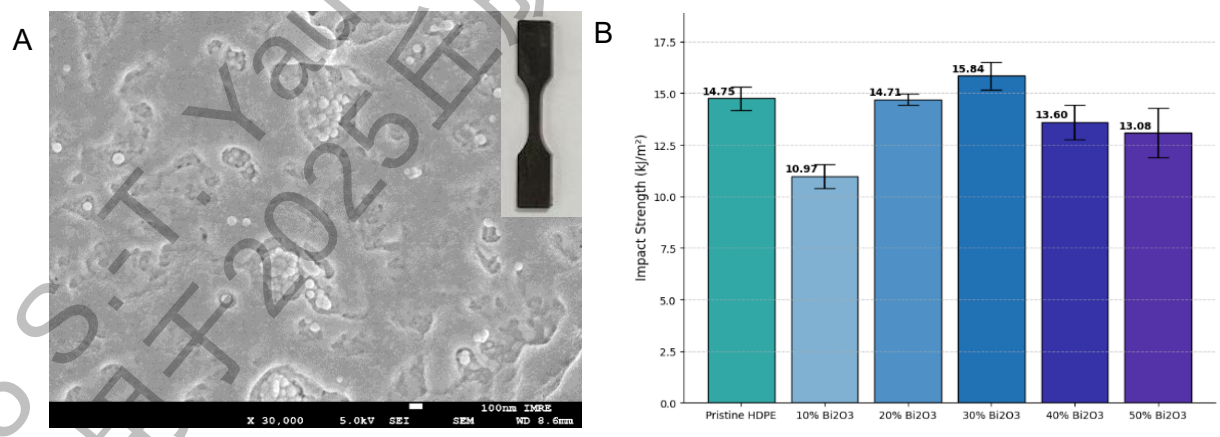

Fig. 6 (A) SEM image of the cross-section of HDPE/Bi tensile bars, showing uniform dispersion of Bi particles within the HDPE matrix. Inset shows a photograph of a HDPE/Bi tensile bar illustrating its

homogeneous appearance. (B) Impact strength comparison of HDPE/Bi composites containing 10–50 wt% Bi_2O_3 relative to the unfilled HDPE control.

The impact strength results (Fig. 6B) reveal a clear composition–property relationship. While low Bi contents (10–20 wt%) provide modest improvements over the unfilled HDPE control, a significant enhancement is observed at 30 wt% Bi, where the composite achieves its highest impact strength. This optimal performance likely arises from the balance between particle reinforcement and matrix ductility at this loading, Bi particles effectively absorb and redistribute impact energy without excessively embrittling the HDPE phase. However, further increasing the filler content to 40–50 wt% results in a decline in impact strength, which can be attributed to particle–particle interactions, reduced polymer chain mobility, and potential microvoid formation at higher filler loadings. Overall, the 30 wt% Bi composition demonstrates the best synergy between toughness and radiation-shielding potential, making it a promising candidate for multifunctional protective materials.

4. Conclusion

We developed a multilayered polymer nanocomposite by synthesizing Bi and Gd_2O_3 nanoparticles *via* a controlled colloidal synthesis process, ensuring precise particle size, morphology, and dispersion. These nanoparticles were incorporated into a HDPE matrix, while ZrO_2 was introduced as an additional reinforcement. The individual nanoparticle–HDPE mixtures were then pelletized and processed using a melt-blown co-extrusion technique, enabling uniform layering into thin, flexible sheets. These sheets form the final nanocomposite material designed for integration into PPE.

This innovation addresses critical challenges in radiation protection by combining high attenuation efficiency with enhanced sustainability. The use of recyclable thermoplastics and non-toxic fillers significantly reduces environmental impact compared to conventional lead-based shields, while the lightweight architecture improves user comfort and mobility. By lowering both the weight and cost of

protective gear, this technology offers a promising pathway for next-generation radiation shielding solutions in medical, nuclear, and aerospace applications. Its potential to reduce occupational health risks, such as radiation-induced cancers and musculoskeletal disorders among healthcare workers, marks a substantial advancement toward safer and more sustainable PPE.

References

1. Oncologist, M. R. B. D. J. T. S. C. R. (2025, January 22). Why radiation therapy is becoming an increasingly common cancer treatment procedure. Dr Johann Tang. https://radiotherapysingapore.com/why-radiation-therapy-is-becoming-an-increasingly-common-cancer-treatment-procedure/
2. International Atomic Energy Agency. (2024, September 30). Optimized radiotherapy approach could extend treatment to 2.2 million more cancer patients, IAEA co-authored report finds. IAEA. https://www.iaea.org/newscenter/pressreleases/optimized-radiotherapy-approach-could-extend-treatment-to-22-million-more-cancer-patients-iaea-co-authored-report-finds
3. Baudin, C., Vacquier, B., Thin, G., Chenene, L., Guersen, J., Partarrieu, I., Louet, M., Ducou Le Pointe, H., Mora, S., Verdun-Esquer, C., Feuardent, J., Rousseau, F., Roy, H., Bensefa-Colas, L., Boyer, L., & Bernier, M.-O. (2023a). Occupational exposure to ionizing radiation in medical staff: Trends during the 2009–2019 period in a multicentric study. European Radiology, 33(8), 5675–5684. https://doi.org/10.1007/s00330-023-09541-z
4. Banaee, N., Goodarzi, K., & Nedaie, H. A. (2021). Neutron contamination in radiotherapy processes: A review study. Journal of Radiation Research, rrab076. https://doi.org/10.1093/jrr/rrab076
5. Bawazeer, O., Makkawi, K., Aga, Z. B., Albakri, H., Assiri, N., Althagafy, K., & Ajlouni, A.-W. (2023). A review on using nanocomposites as shielding materials against ionizing radiation. Journal of Umm Al-Qura University for Applied Sciences, 9(3), 325–340. https://doi.org/10.1007/s43994-023-00042-9
6. Bijanu, A., Arya, R., Agrawal, V., Tomar, A. S., Gowri, V. S., Sanghi, S. K., Mishra, D., & Salammal, S. T. (2021). Metal-polymer composites for radiation protection: A review. Journal of Polymer Research, 28(10), 392. https://doi.org/10.1007/s10965-021-02751-3
7. Development of Lead-Free Materials for Radiation Shielding in Medical Settings: A Review. (2024). Journal of Biomedical Physics and Engineering. https://doi.org/10.31661/jbpe.v0i0.2404-1742
8. Chang, Q., Guo, S., & Zhang, X. (2023). Radiation shielding polymer composites: Ray-interaction mechanism, structural design, manufacture, and biomedical applications. Materials & Design, 233, 112253. https://doi.org/10.1016/j.matdes.2023.112253

9. Jain, S. (2021). Radiation in medical practice & health effects of radiation: Rationale, risks, and rewards. Journal of Family Medicine and Primary Care, 10(4), 1520–1524. https://doi.org/10.4103/jfmpc.jfmpc_2292_20

10. Echeweozo, E., Kırkbınar, M., Alomairy, S., & Al-Buriahi. (2024). Gamma radiation and charged particle shielding properties of Polymethyl methacrylate- Bi2O3 composite for medical shielding applications: Synthesis and simulation study. Journal of Radiation Research and Applied Sciences, 18(1), 101247. https://doi.org/10.1016/j.jrras.2024.101247
11. Wang, K.; Ma, L.; Yang, C.; Bian, Z.; Zhang, D.; Cui, S.; Wang, M.; Chen, Z.; Li, X. Recent Progress in Gd-Containing Materials for Neutron Shielding Applications: A Review. Materials 2023, 16, 4305. https://doi.org/10.3390/ma16124305
12. Sayyed, M. I., Mahmoud, K. A., & Hanafy, T. A. (2025). A new protective glass material against gamma ray: Thorough analysis to determine the impact of adding gadolinium (III) oxide. Nuclear Engineering and Technology, 57(1), 103146. https://doi.org/10.1016/j.net.2024.08.015
13. Bannunah, A. M. (2023). Biomedical Applications of Zirconia-Based Nanomaterials: Challenges and Future Perspectives. Molecules, 28(14), 5428. https://doi.org/10.3390/molecules28145428
14. Fontainha, C. C. P., Baptista Neto, A. T., Santos, A. P., & Faria, L. O. D. (2016). P(VDF-TrFE)/ZrO2 Polymer-Composites for X-ray Shielding. Materials Research, 19(2), 426–433. https://doi.org/10.1590/1980-5373-MR-2015-0576
15. Alhindawy, I. G., Marashdeh, Mohammad. W., Aljaafreh, Mamduh. J., Al-Hmoud, M., Alanazi, S., & Mahmoud, K. (2024). Advanced radiation shielding materials: PbO2-doped zirconia ceramics synthesized through an innovative sol-gel method. Nuclear Engineering and Technology, 56(7), 2444–2451. https://doi.org/10.1016/j.net.2024.02.001
16. Nabiyev, A. A., Olejniczak, A., Islamov, A. Kh., Pawlukojc, A., Ivankov, O. I., Balasoiu, M., Zhigunov, A., Nuriyev, M. A., Guliyev, F. M., Soloviov, D. V., Azhibekov, A. K., Doroshkevich, A. S., Ivanshina, O. Yu., & Kuklin, A. I. (2021). Composite Films of HDPE with SiO2 and ZrO2 Nanoparticles: The Structure and Interfacial Effects. Nanomaterials, 11(10), 2673. https://doi.org/10.3390/nano11102673